



**HAL**  
open science

## Clean hydrogen production by the hydrolysis of magnesium-based material: Effect of the hydrolysis solution

Serge Al Bacha, Anne Thienpont, Mirvat Zakhour, Michel Nakhl, Jean-Louis Bobet

### ► To cite this version:

Serge Al Bacha, Anne Thienpont, Mirvat Zakhour, Michel Nakhl, Jean-Louis Bobet. Clean hydrogen production by the hydrolysis of magnesium-based material: Effect of the hydrolysis solution. *Journal of Cleaner Production*, 2021, 282, pp.124498. 10.1016/j.jclepro.2020.124498 . hal-03097935

**HAL Id: hal-03097935**

**<https://hal.science/hal-03097935>**

Submitted on 5 Jan 2021

**HAL** is a multi-disciplinary open access archive for the deposit and dissemination of scientific research documents, whether they are published or not. The documents may come from teaching and research institutions in France or abroad, or from public or private research centers.

L'archive ouverte pluridisciplinaire **HAL**, est destinée au dépôt et à la diffusion de documents scientifiques de niveau recherche, publiés ou non, émanant des établissements d'enseignement et de recherche français ou étrangers, des laboratoires publics ou privés.

# Clean hydrogen production by the hydrolysis of Magnesium-based material: effect of the hydrolysis solution

S. Al Bacha <sup>a,b</sup>, A. Thienpont <sup>c</sup>, M. Zakhour <sup>a</sup>, M. Nakhl <sup>a</sup>, J.-L. Bobet <sup>b\*</sup>.

<sup>a</sup> LCPM/PR<sub>2</sub>N (EDST), Lebanese University, Faculty of Sciences II, 90656 Jdeidet El Metn, Liban.

<sup>b</sup> University of Bordeaux, ICMCB, CNRS, UMR 5026, F-33600 Pessac, France.

<sup>c</sup> University of Bordeaux, ISM, UMR 5255, 351 cours de la Libération, F-33405 Talence, France.

## Abstract

Autonomous low-pressure hydrogen on demand system was found promising to supply fuel cell technology for light or short distance mobility applications. Among the various hydrogen production technologies, the hydrolysis reaction method of magnesium-based materials is one of the most suitable. Magnesium (Mg) powder ball milled with the simultaneous addition of graphite and nickel under Ar was used as the hydrolysis reagent for hydrogen production. The effects of the solution composition (*i.e.* NaCl, NH<sub>4</sub>Cl and HCl) and the temperature (*i.e.* from 0°C to 60°C) of the solution on the hydrolysis performances were discussed. The hydrolysis reaction was complete (*i.e.* yield = 100%) in less than 5 minutes, except that performed at 0°C, regardless the hydrolysis solution. The activation energy of the reaction decreases with lowering the pH of the hydrolysis solution. Semi-quantitative analysis was performed to evaluate the variation of CH<sub>4</sub>, CO, CO<sub>2</sub> and moisture contents in the hydrogen produced by the hydrolysis. The exothermicity of the reaction and the composition of the hydrolysis solution showed a major impact on the purity of hydrogen. Under standard pressure and ambient temperature conditions, the hydrolysis of magnesium-based materials is considered as a clean hydrogen production technique. Our results should be taken as the starting point to evaluate the purity of the hydrogen produced by the hydrolysis of Mg-based materials according to the ISO standard 14687:2019.

**Keywords:** Hydrogen production, Hydrolysis, Humidity, CO<sub>2</sub>, Magnesium, Clean hydrogen.

\* corresponding author: [jean-louis.bobet@icmcb.cnrs.fr](mailto:jean-louis.bobet@icmcb.cnrs.fr) (J.-L. Bobet)

# 1. Introduction

The technological revolution, the continuous growth of both the population and the world economy increase drastically the energy demand (Radcliffe, 2018). As a consequence, energy issue has become a key point of our daily life and a need to almost all human activities (Abe et al., 2019). Nowadays, fossil fuels such as petroleum, natural gas and coal provide more or less 80% of all the energy consumed worldwide (Rusman and Dahari, 2016). World energy consumption is expected to reach a peak in 2035 while the world economy could enter a long period of depression around 2020 (Rand, 2011; Rusman and Dahari, 2016). Moreover, current fossil fuel reserves are supposed to support a maximum of 40 years for petroleum, 60 years for natural gas and 156 years for coal (Midilli et al., 2005). In addition, considering the energy production from fossil fuels since the industrial revolution, a massive emission of carbon dioxide (CO<sub>2</sub>) and other greenhouse gases (*e.g.* CO, NO, NO<sub>2</sub>, ...) in the atmosphere is evidenced causing the global warming (Dawood et al., 2020). The world's shift away from the fossil fuel economy toward a much cleaner energy production system is essential for future energy sustainability, global security and climate change (Durbin and Malardier-Jugroot, 2013; Rand, 2011). Renewable energy resources will play a key role in the transition to a clean and "green" energy system (Marbán and Valdés-Solís, 2007; Midilli et al., 2005). In this context, dihydrogen gas (H<sub>2</sub>) as an energy carrier is among the most promising solutions for the next generation energy economy (Abe et al., 2019; Dawood et al., 2020; Mazloomi and Gomes, 2012). The hydrogen-based energy system comprises four main stages; production (including purification and transport), storage, safety and utilization (Dawood et al., 2020). Considering the main uses, hydrogen can be considered to power an internal combustion engine or a fuel cell (*e.g.* PEMFC) (Marbán and Valdés-Solís, 2007). The International Organization for Standardization listed, in standard ISO 14687:2019, the specifications for hydrogen gas (Type I) as a fuel for internal combustion engines (Grade A), for fuel cells used in road vehicles (Grade D) and for stationary appliances (Grade E-3)(ISO, 2019).

One of the main challenges of the transition to the "hydrogen" energy is its unavailability in nature (abundant in the combined state) and the need to optimize eco-friendly and inexpensive production methods. Hydrogen can be extracted from fossil fuels, biomass, renewable resources and water (Abdin et al., 2020; Abe et al., 2019; Dawood et al., 2020; Dincer, 2012; Mazloomi

1 and Gomes, 2012; Nikolaidis and Poullikkas, 2017). The emission of carbon byproduct (*e.g.* CO<sub>2</sub>,  
2 CO, tar aerosol, ...) during the hydrocarbon reforming (*i.e.* steam reforming, partial oxidation,  
3 autothermal steam reforming) involve research to develop alternative production techniques  
4 (Nikolaidis and Poullikkas, 2017). The major disadvantages of hydrogen production from  
5 biomass (*i.e.* pyrolysis, gasification, bio-photolysis, fermentation, ...) remain the seasonal  
6 availability, the dioxygen gas (O<sub>2</sub>) sensitivity and the low efficiency. The conventional process  
7 to extract hydrogen by water splitting (*i.e.* electrolysis and thermolysis) needs relatively  
8 important infrastructures and high capital costs in addition to corrosive problems. “Green”  
9 hydrogen production describes the procedures where the energy produced (*i.e.* thermal, electrical,  
10 biochemical and photonic) from renewable resources (*i.e.* solar, geothermal, wind, ...) is used to  
11 generate hydrogen either from biomass or by water splitting (Dincer, 2012).

12 In contrast, storage of hydrogen is a primary issue enabling technology for hydrogen energy  
13 systems development. Hydrogen can be stored in gaseous state, liquid state or in solid metal  
14 hydrides (Abe et al., 2019; Seyam et al., 2020). However, the storage system must meet certain  
15 requirements, in particular a low operating pressure and temperature, a multicyclic reversibility  
16 and rapid kinetics of hydrogen absorption / desorption, stability against oxygen and humidity and  
17 low cost of recycling and charging infrastructure system (Acar and Dincer, 2019; Durbin and  
18 Malardier-Jugroot, 2013).

19 Hydrogen on demand (HOD) generation system is a promising solution for clean energy  
20 production (Mauvy et al., 2019; Potapov et al., 2019; Sabatier et al., 2018). Using the hydrogen  
21 produced directly to power a fuel cell (*e.g.* Proton-Exchange Membrane Fuel cell (PEMFC))  
22 solves both the hydrogen supply and storage problems offering a suitable system for low power  
23 applications as well as light or short distance mobility applications. This HOD generator is based  
24 on the hydrolysis reaction of magnesium-based materials (Mg) (Xie et al., 2020). This method is  
25 promising since the reaction occurs spontaneously at normal conditions of pressure and  
26 temperature. Unfortunately, the quickly formed magnesium hydroxide layer hinders the  
27 interaction between Mg and water which reduces hydrogen generation performances (*i.e.* yield  
28 and kinetics) (Tayeh et al., 2014).

1 Recently, a large-scale hydrogen supply test of Mg milled with 5 wt.% of expanded graphite was  
2 carried out via an HOD system (Ma et al., 2019). The results reported by Ma *et al.* (Ma et al.,  
3 2019) showed that this material is very promising for efficient low-cost hydrogen production  
4 with a maximum hydrogen generation rate of 12.3 L.min<sup>-1</sup> and a hydrolysis yield of 94% in 3  
5 minutes.

6 Among the Mg-based mixtures elaborated for enhancing the hydrolysis reaction, Mg ball milled  
7 under hydrogen with the simultaneous addition of 5 wt.% of nickel (Ni) and 5 wt.% of graphite  
8 (G) (subsequently named Mg-Ni-G) showed the best performances with a complete hydrolysis  
9 reaction in less than few minutes (Awad et al., 2016) due to the formation of a protective layer  
10 which hinder the adhesion of the formed Mg(OH)<sub>2</sub> (effect of graphite (Al Bacha et al., 2019;  
11 Awad et al., 2016; Fuster et al., 2011)), the modification of the microstructural properties of Mg  
12 powder and the establishment of micro-galvanic cell between Mg and Ni which improve the  
13 galvanic corrosion (effect of Ni (Al Bacha et al., 2019; Grosjean et al., 2005; Grosjean et al.,  
14 2006; Kravchenko et al., 2014)). In our previous study, powder milling under Ar was found to be  
15 more suitable for industrial application and more efficient than that under H<sub>2</sub> atmosphere, in term  
16 of hydrolysis performances, due to the formation of less reactive MgH<sub>2</sub> (Al Bacha et al., 2020b;  
17 Al Bacha et al., 2020c). Consequently, Mg-Ni-G was ball milled under Ar for better hydrolysis  
18 reactivity. On the other hand, several studies have reported the hydrolysis of magnesium-based  
19 materials (*i.e.* Mg and MgH<sub>2</sub>) in chlorides solutions showing the beneficial effect of chloride ions  
20 (Cl<sup>-</sup>) (Al Bacha et al., 2020a; Al Bacha et al., 2020b; Al Bacha et al., 2020c; Grosjean and Roué,  
21 2006; Grosjean et al., 2005) as well as acidic solutions (MgCl<sub>2</sub> (Buryakovskaya et al., 2019;  
22 Pighin et al., 2020 ; Tan et al., 2018), AlCl<sub>3</sub> (Buryakovskaya et al., 2019), citric acid (Hiraki et  
23 al., 2012; Kushch et al., 2011; Uan et al., 2009; Yu et al., 2012), acetic acid (Öz et al., 2017; Yu  
24 et al., 2012), NH<sub>4</sub>Cl (Huang et al., 2015)). Recently, Tan *et al.* (Tan et al., 2019) analyzed the  
25 purity of the hydrogen produced by the hydrolysis of Mg<sub>2</sub>Si in NH<sub>4</sub>F and NH<sub>4</sub>Cl to highlight the  
26 beneficial effect of F<sup>-</sup> anions on suppressing the formation of the “explosive” silane. However, in  
27 these studies, the effect of the composition of the hydrolysis solution and its temperature on the  
28 purity of the produced hydrogen was not reported. It is mandatory to evaluate the effect of the  
29 hydrolysis conditions (*e.g.* hydrolysis solution, reaction temperature, Mg/water ratio) not only on  
30 the hydrogen generation performances (as reported in the literature) but on the purity of the  
31 formed fuel.

1 In this study, the effect of the hydrolysis solution (*i.e.* NaCl, NH<sub>4</sub>Cl and HCl) on the hydrolysis  
2 performances of Mg-Ni-G with estimating the activation energies using Avrami-Erofeev model  
3 are examined. The effect of the exothermicity of the reaction as well as the composition of the  
4 hydrolysis solution on the humidity and the purity of the gas mixture, in term of CO<sub>2</sub> footprint,  
5 generated during the hydrolysis are also investigated. Our results show the best experimental  
6 conditions for a clean hydrogen production based on the hydrolysis reaction of Mg-based  
7 materials.

8

## 9 **2. Experimental details**

10 Magnesium powder (Strem Chemicals, 99.8%) was ball milled with 5 wt.% of nickel powder  
11 (Alfa Aesar, 99.5%) and 5 wt.% of graphite powder (Fischer Scientific) in a Fritsch Pulverisette  
12 7 under 5 bar of Ar atmosphere. Milling was performed at 250 rpm with the sequence of 15  
13 minutes of continuous milling followed by 2 minutes of rest and a ball to powder weight ratio of  
14 17:1. Powder was passed through a sieve of 200 µm and stocked in a glove box filled with  
15 purified argon.

16 Materials before and after hydrolysis were analyzed by X-ray diffraction (Philips  
17 PANalyticalX'Pert (PW1820) diffractometer with Cu K $\alpha$ 1 radiation ( $\lambda=1.5405\text{\AA}$ )), laser  
18 granulometry in absolute ethanol (MASTERSIZER 2000 from Malvern ®) and scanning  
19 electron microscopy (TESCAN VEGA3 SB). Hydrolysis tests were carried using a homemade  
20 setup previously described in 0.6 mol/L aqueous chloride solution prepared by mixing NaCl  
21 (UNI-CHEM, 99.8%), NH<sub>4</sub>Cl (Sigma Aldrich, 99.9%) or HCl (Sigma Aldrich, 37%) with pure  
22 deionized water. The tests were repeated at least three times for better reproducibility.

23 The gas mixture produced by the hydrolysis was collected in Tedlar® gas sampling bags (Sigma  
24 Aldrich, *Cf* Supplementary materials Figure S1) and analyzed using a VARIAN (CP-4900 PRO)  
25 micro-gas chromatograph (GC, *Cf* Supplementary materials Figure S2) equipped with two  
26 columns in parallel: a CP-Molsieve 5A, 10 m and a CP-PoraPLOT Q, 10 m (subsequently  
27 named MS and PPQ respectively). MS column heated at 90°C with pure Ar as carrier gas allows  
28 the separation of permanent gases such as H<sub>2</sub>, N<sub>2</sub>, O<sub>2</sub>, CH<sub>4</sub> and CO while volatile hydrocarbons

1 C<sub>2</sub>-C<sub>6</sub>, CO<sub>2</sub>, H<sub>2</sub>S, SO<sub>2</sub> are separated using the PPQ column heated at 70 °C with pure He as  
2 carrier gas. Upstream of each column, a protective column prevents the passage of incompatible  
3 gases with the selected column (Supplementary materials Figure S3). For instance, the stationary  
4 phase of the protection column allows the retention of water, CO<sub>2</sub> and hydrocarbons, which  
5 prevents their injection into the MS column. Separated gases were detected using a thermal  
6 conductivity detector (TCD). Each gas mixture analysis was repeated 5 times with a sample loop  
7 of 10 µL.

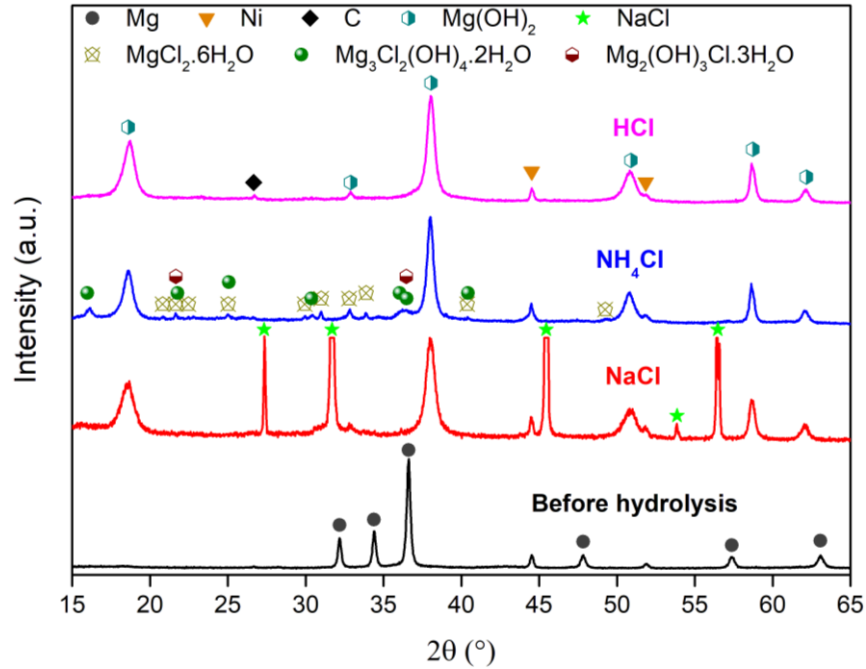
8 The moisture in the gas produced by the hydrolysis of Mg was evaluated using a humidity and  
9 temperature transmitters DO 9861T (Delta Ohm) psychrometer at room temperature  
10 (Supplementary materials Figure S4). The system was purged with pure argon before each  
11 measurement until minimal absolute humidity of 0.08 g/m<sup>3</sup> was reached.

12

### 13 **3. Results and discussion**

#### 14 *3.1. Hydrogen generation*

15 The improvement in the hydrolysis performances of Mg depends on the success in disrupting the  
16 formation of the passivation layer. Magnesium hydroxide Mg(OH)<sub>2</sub> (solubility = 0.00178 g/L in  
17 pure water at 20°C) is formed when the concentration of Mg<sup>2+</sup> ions reaches 7 mmol/L (Hiraki et  
18 al., 2012). Chloride ions promote the formation of water soluble MgCl<sub>2</sub> (s = 468.7 g/L in pure  
19 water at 20°C) which forms water channels through the passivation layer and prevents the small  
20 dispersed Mg(OH)<sub>2</sub> particles adhesion to Mg particles (Awad et al., 2016). Furthermore,  
21 according to Pourbaix diagram of the magnesium-water system (Pourbaix, 1974), lowering the  
22 pH increases the solubility of Mg(OH)<sub>2</sub> which enhances the hydrolysis performances.

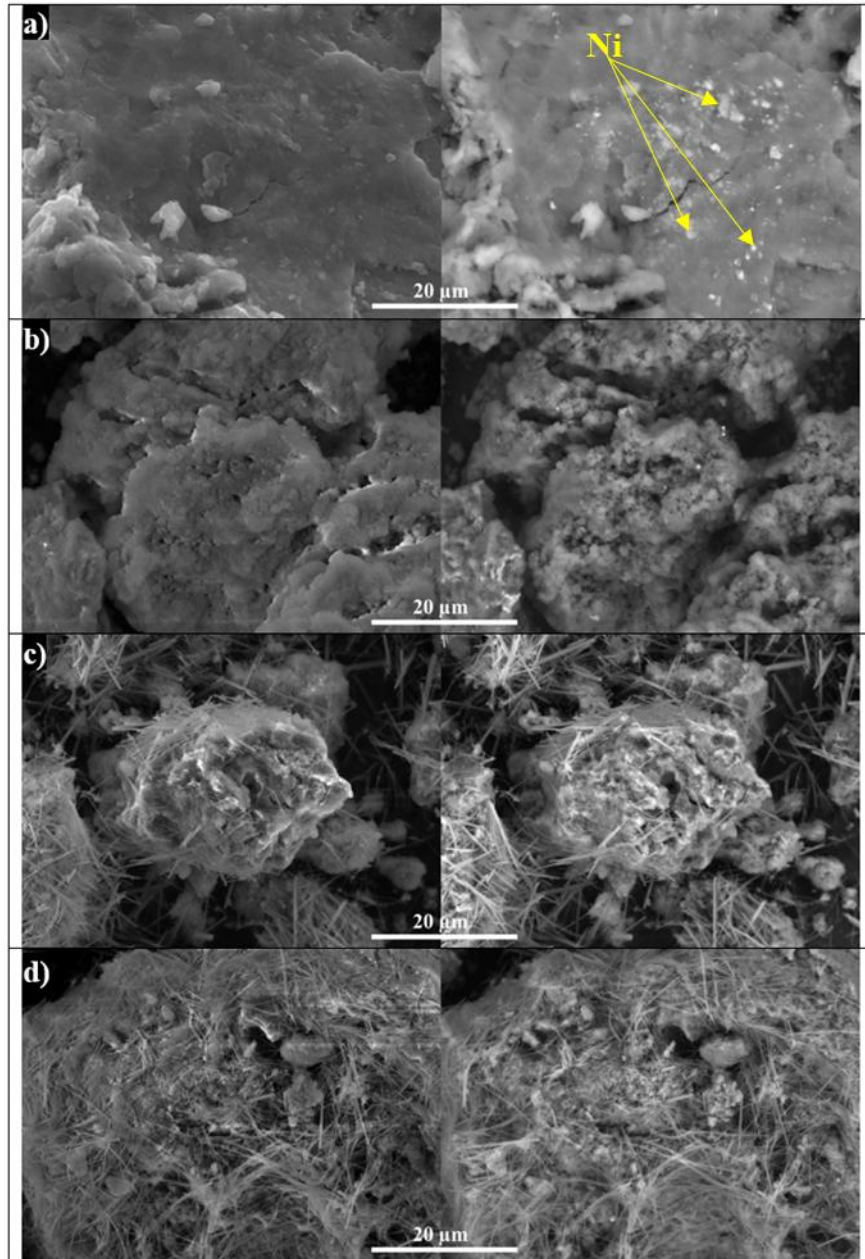


1

2 Figure 1: XRD patterns of Mg-Ni-G before hydrolysis and after hydrolysis in NaCl, NH<sub>4</sub>Cl and HCl  
 3 solutions.

4

5 X-ray diffraction patterns of Mg ball milled under Ar for 3h with the simultaneous addition of 5  
 6 wt.% of Ni and 5 wt.% of G (Figure 1) shows the presence of Mg (Powder Diffraction File PDF:  
 7 00-035-0821) without any preferential orientation along the *c*-axis and the presence of Ni (PDF:  
 8 00-004-0850) while the absence of peaks of graphite (PDF: 00-056-0159) can be assigned to its  
 9 amorphisation during ball milling as previously reported (Al Bacha et al., 2019; Al Bacha et al.,  
 10 2020b; Al Bacha et al., 2020c). No chemical reaction (*e.g.* mechanical alloying) occurs between  
 11 Mg, Ni metal and carbon graphite (G) since only the diffraction peaks of pure elements are  
 12 observed.

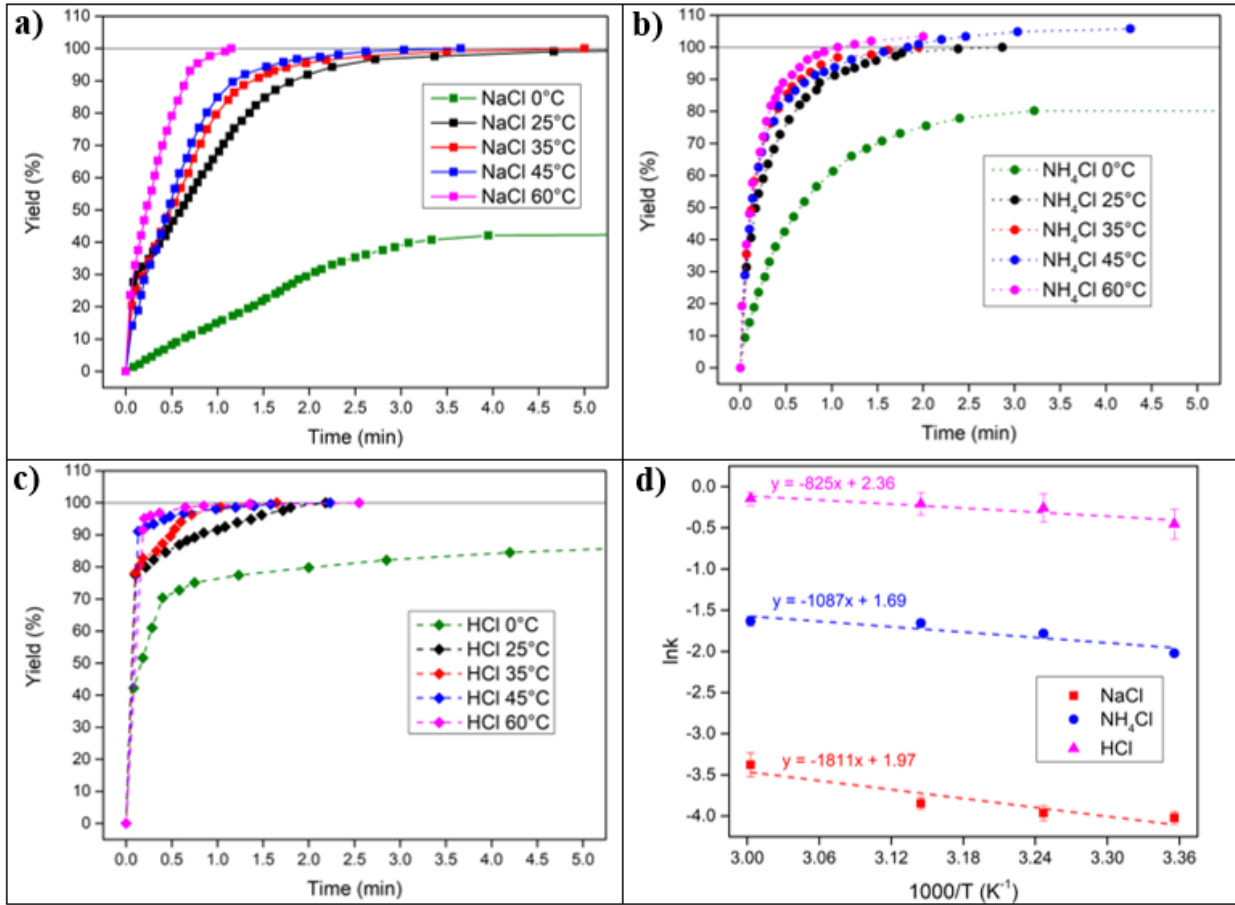


1  
 2 Figure 2: SE (left) and BSE (right) images of Mg-Ni-G: a) before hydrolysis, b) after hydrolysis in NaCl,  
 3 c) after hydrolysis in  $\text{NH}_4\text{Cl}$  and d) after hydrolysis in HCl.

4

5 The presence of metallic elements as ball milling additives improves the efficiency of the milling  
 6 process by creating microstructural defects and reducing particles size (Al Bacha et al., 2019;  
 7 Awad et al., 2016; Grosjean et al., 2005). Laser granulometry measurements show that particles  
 8 size decrease from 54  $\mu\text{m}$  to 19  $\mu\text{m}$  after ball milling while BSE mode micrographs reveal the

1 presence of Ni particles (white stains implying different chemical composition) on the surface of  
 2 Mg (Figure 2.a).



3  
 4 Figure 3: Hydrogen generation by the hydrolysis of Mg-Ni-G at various temperatures in: a) NaCl  
 5 solution, b) NH<sub>4</sub>Cl solution<sup>1</sup>, c) HCl solution and d) Kissinger plot.

6  
 7 Hydrogen generation by the hydrolysis of Mg-Ni-G was carried out using 0.6 mol/L NaCl (*i.e.*  
 8 average concentration of NaCl in seawater (*i.e.* 3.5wt.%, Figure 3.a), 0.6 mol/L NH<sub>4</sub>Cl (Figure  
 9 3.b) and 0.6 mol/L HCl (Figure 3.c) at various temperature (*e.g.* 0°C, 25°C, 35°C, 45°C and  
 10 60°C).

<sup>1</sup> the excess of hydrogen production (*i.e.* yield > 100%) when the hydrolysis is performed in NH<sub>4</sub>Cl is attributed to the evaporation of NH<sub>3</sub> from the hydrolysis solution.

1 As expected, hydrolysis performances are enhanced by increasing reaction media temperature  
2 from 0°C to 60°C of each of the chloride solution. Apart the hydrolysis test carried out at 0°C,  
3 total hydrolysis reactions (*i.e.* production of 889 mL.g<sup>-1</sup> corresponding to a yield of 100%) are  
4 reached in less than 5 minutes. Pure Mg produced 98.7 mL.g<sup>-1</sup> (corresponding to 10% of its  
5 theoretical H<sub>2</sub> production capacity) within 5 minutes of hydrolysis in 3.5 wt.% NaCl solution at  
6 25°C (Awad et al., 2016). At 25°C, the average hydrogen generation rate increase from 196  
7 mL.min<sup>-1</sup>.g<sup>-1</sup> to 317 mL.min<sup>-1</sup>.g<sup>-1</sup> and 553 mL.min<sup>-1</sup>.g<sup>-1</sup> by substituting NaCl with NH<sub>4</sub>Cl and HCl  
8 solutions respectively (Supplementary materials Table S1). For instance, while rising the  
9 temperature of NaCl solution from 0°C to 60°C, hydrogen generation becomes faster with an  
10 average production rate varying from 98 mL.min<sup>-1</sup>.g<sup>-1</sup> to 320 mL.min<sup>-1</sup>.g<sup>-1</sup> while in HCl a  
11 maximum generation rate of 786 mL.min<sup>-1</sup>.g<sup>-1</sup> was estimated (Supplementary materials Table S1).  
12 Huang *et al.* (Huang et al., 2017) reached an average hydrogen generation rate of approximately  
13 160 mL.min<sup>-1</sup>.g<sup>-1</sup> (the mass of the additive is included in the calculations) in 5 minutes of  
14 hydrolysis of Mg milled with 10 wt.% of MoS<sub>2</sub> at 25°C. In fact, rapid hydrogen generation is one  
15 of the advantages for the *in-situ* hydrogen on demand system so that the hydrogen is released  
16 directly when the solution is mixed with the powder. The improvement in the reaction kinetics  
17 with the temperature is attributed to:

- 18 (i) the vibrational energy of water that increases with the temperature. It inhibits the  
19 thickening and the accumulation of the passivation layer of magnesium hydroxide  
20 Mg(OH)<sub>2</sub> on fresh Mg surface,  
21 (ii) the solubility of Mg(OH)<sub>2</sub> which increases when increasing the temperature following  
22 the equation:

$$\ln K_s = A + \frac{B}{T} + C \times \ln T \quad (1)$$

23 where K<sub>s</sub> is the solubility constant, A, B and C are experimental parameters and T is  
24 temperature in K (Pinsky and Takano, 2004).

25 On the other side, the hydrolysis solution composition has a major impact on the hydrolysis  
26 performances of Mg-Ni-G. The three solutions share the same concentration of Cl<sup>-</sup> ions (*i.e.* 0.6  
27 M) so that the effect of the solution cation can be identified. As previously reported (Al Bacha et  
28 al., 2020d), the pH decrease is expected to raise the solubility of Mg(OH)<sub>2</sub> according to

1 Henderson-Hasselbalch equation with increasing concentration of the ionized species. The  
2 reaction kinetics are maximal when using HCl solution while they decrease with NH<sub>4</sub>Cl and  
3 NaCl respectively (Figures 3.c, 3.b and 3.a respectively). These results can be explained by the  
4 strength of the considered acid. Indeed, HCl is a strong acid while NH<sub>4</sub>Cl is a weak acid.

5 Figure 3.b shows that the hydrogen production in NH<sub>4</sub>Cl exceeds the theoretical generated  
6 hydrogen volume calculated using the hydrolysis equation of Mg (*i.e.* yield > 100% and the total  
7 H<sub>2</sub> volume exceeds 919 mL.g<sup>-1</sup> and 940 mL.g<sup>-1</sup> at 45°C and 60°C respectively). In fact, NH<sub>4</sub>Cl  
8 dissolution generates HCl and NH<sub>3</sub> in the reaction media following the dissolution reaction:



9 considering that the enthalpy and the entropy of the reaction are constant in the temperature  
10 range (0°C to 60°C).

11 The very low Gibbs Energy ( $\Delta_r G$ ) needed to evaporate ammonia gas NH<sub>3</sub> (according to reaction  
12 2) can be easily supplied from the hydrolysis reaction which is exothermic. Consequently, it will  
13 induce an increase of the volume of the generated gases (*i.e.* H<sub>2</sub> + NH<sub>3</sub>).

14 After the hydrolysis tests, the reaction media (Mg-Ni-G + hydrolysis solution) was dried  
15 overnight at 100°C under air. XRD patterns of the solid products (Figure 1) after hydrolysis  
16 shows that all Mg has reacted to form magnesium hydroxide (PDF: 00-044-1482) after the  
17 hydrolysis in NaCl, NH<sub>4</sub>Cl and HCl solutions. Magnesium chloride (PDF: 00-025-0515) and  
18 magnesium oxychloride (*i.e.* xMg(OH)<sub>2</sub> + yMgCl<sub>2</sub> in aqueous solution; *e.g.* Mg<sub>2</sub>(OH)<sub>3</sub>Cl.3H<sub>2</sub>O  
19 (PDF:00-007-0403) and Mg<sub>3</sub>Cl<sub>2</sub>(OH)<sub>4</sub>.2H<sub>2</sub>O (PDF:00-012-0133)) were formed after the reaction  
20 in NH<sub>4</sub>Cl solution. The dissociation of NH<sub>4</sub>Cl (implying the production of NH<sub>3</sub>) is demonstrated  
21 in Figure 1 where the XRD diffractogram of Mg-Ni-G after the hydrolysis in NH<sub>4</sub>Cl does not  
22 show peaks attributed to NH<sub>4</sub>Cl (PDF: 00-002-0887). Conversely, peaks attributed to NaCl  
23 (PDF:00-005-0628) are observed in the XRD diffractogram of Mg-Ni-G after the hydrolysis in  
24 NaCl.

25 Particles size (estimated by laser granulometry measurements) decreases from 19 μm (before  
26 hydrolysis) to 3 μm, 1 μm and 5 μm after hydrolysis in NaCl, NH<sub>4</sub>Cl and HCl media  
27 respectively. The morphology of the materials changes significantly after the hydrolysis. After

1 reaction in NaCl, the smaller particles tend to agglomerate (Figure 2.b) while after the reaction in  
 2 NH<sub>4</sub>Cl (Figure 2.c) and HCl (Figure 2.d), needle-like structure is observed. This structure type  
 3 was previously reported for magnesium oxychloride cements (Qu et al., 2020).

4 The hydrogen production by the hydrolysis of Mg-based materials follows the nucleation and  
 5 growth mechanism modeled by Avrami-Erofeev equation (Tan et al., 2020):

$$\alpha(t) = 1 - e^{-kt^n} \quad (3)$$

6 where  $\alpha(t)$  is the reaction rate, *i.e.* the hydrolysis yield,  $k$  is the reaction rate coefficient,  $n$  is a  
 7 constant that depends on the mechanism, and  $t$  is reaction time.  $n$  values characterize the  
 8 diffusion process where a value near 0.62 determines a one-dimensional diffusion process while  
 9 a value close to 1.07 is characteristic of a three-dimensional interface reaction process (Hou et al.,  
 10 2019; Liu et al., 2009). In the present study, the observed average values of  $n$  are close to 1.06,  
 11 0.7 and 0.41 for the hydrolysis of Mg-Ni-G in NaCl, NH<sub>4</sub>Cl and HCl respectively implying a  
 12 change on the diffusion mode : the hydrogen production process of Mg-Ni-G in NaCl seems to  
 13 be controlled by the three-dimensional interface reaction while the mechanism of the hydrolysis  
 14 in NH<sub>4</sub>Cl (and by default the one in HCl) could be a one-dimensional diffusion-controlled  
 15 reaction.

16 The hydrolysis activation energy ( $E_A$ ) is estimated using the Arrhenius equation:

$$k = A \cdot e^{-\frac{E_A}{RT}} \quad (4)$$

17 where  $A$  is the pre-exponential factor of the reaction,  $R$  is the molar gas constant and  $T$  is the  
 18 hydrolysis media temperature (K). The activation energy represents the minimal energy for a  
 19 reaction to occur. An active catalyst reduces the activation energy which enhance the reaction  
 20 performances. For instance, the decrease in  $E_A$  values for the hydrolysis of Mg-based materials  
 21 means higher hydrolysis performances (Awad et al., 2016).

22

23 Table 1: Kissinger plot equations and activation energy values calculated from the best fit of the  
 24 experimental results of the hydrolysis of Mg – Ni – G in NaCl, NH<sub>4</sub>Cl and HCl solutions.

Hydrolysis solution	Equation	$E_A$ (kJ/mol)*	$R^2$
NaCl	$y = -1811x + 1.97$	$15.1 \pm 4.1$	0.8056
NH <sub>4</sub> Cl	$y = -1087x + 1.69$	$9.0 \pm 2.8$	0.7573

HCl	$y = -825x + 2.36$	$6.9 \pm 1.9$	0.7994
-----	--------------------	---------------	--------

1 \* the high uncertainty on the activation energy values is attributed to the narrow temperature range from  
2 0°C to 60°C even if the experimental values of  $\ln k$  fit the Arrhenius equation (Figure 3.d).

3

4 The fit of the experimental data to the Arrhenius equation (*i.e.* Kissinger plots) is represented in  
5 Figure 3.d and Table 1. Activation energy results are in good agreement with the activation  
6 energy of Mg-Ni-G reported by Awad *et al.* (Awad *et al.*, 2016) (14.34 kJ/mol) even though the  
7 milling conditions are different (*i.e.* in the present study, Mg-Ni-G is elaborated by ball milling  
8 under Ar for 3h while in reference (Awad *et al.*, 2016) ball milling was performed under H<sub>2</sub> for  
9 1h). Hydrolysis performances improvement can be assigned to the effect of H<sub>3</sub>O<sup>+</sup> cation (pH  
10 (HCl) < pH (NH<sub>4</sub>Cl) < pH (NaCl)) which favors the dissolution of the passivation layer. The  
11 activation energies vary as the pH of the solutions (*i.e.*  $E_A(\text{HCl}) < E_A(\text{NH}_4\text{Cl}) < E_A(\text{NaCl})$ ) and  
12 inversely to the hydrolysis kinetics. This result confirms that the hydrolysis rate is only limited  
13 by the formation of the passivation layer of MgO/Mg(OH)<sub>2</sub>.

14

### 15 3.2. Gas Analysis

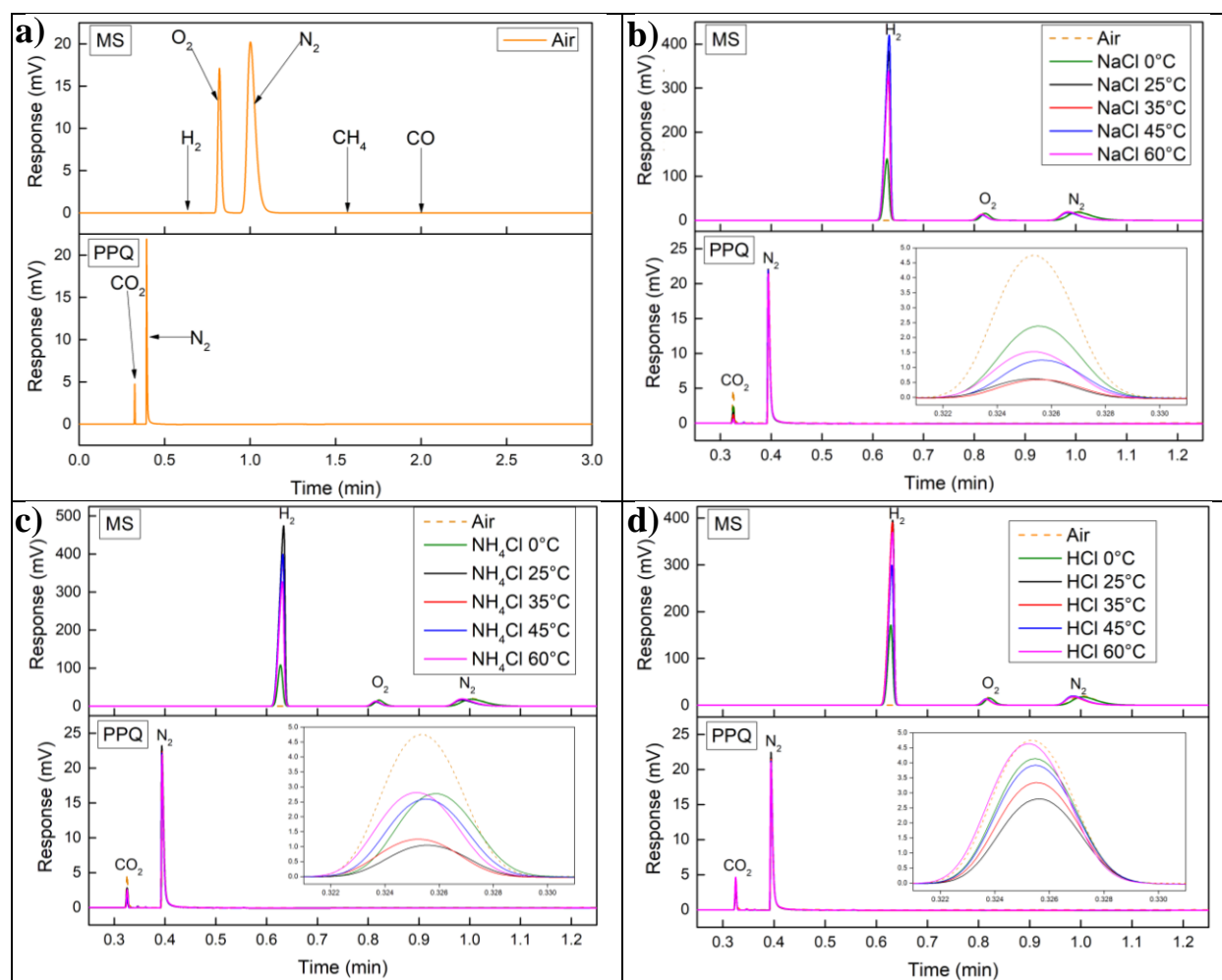
16 Out of the 13 gaseous contaminants specified in ISO 14687:2019 (ISO, 2019), only few are  
17 likely to be present in the hydrogen produced by Mg hydrolysis namely CH<sub>4</sub>, CO, CO<sub>2</sub>, NH<sub>3</sub>, N<sub>2</sub>,  
18 O<sub>2</sub> and moisture (H<sub>2</sub>O). The permitted limits (PL) of each of these contaminants, as listed in ISO  
19 standard depend on the application of hydrogen (Type I, Grades A, D and E-3). On one hand, the  
20 PL for these impurities in H<sub>2</sub> type I (regardless their grade) are as follow: 100 μmol/mol for CH<sub>4</sub>,  
21 0.2 μmol/mol for CO, 2 μmol/mol for CO<sub>2</sub> and 0.1 μmol/mol for NH<sub>3</sub>. On the other hand the PL  
22 for N<sub>2</sub>, O<sub>2</sub> and H<sub>2</sub>O depend on the grade of H<sub>2</sub> : 300 μmol/mol for N<sub>2</sub> in H<sub>2</sub> Grade A and B *vs.*  
23 300 μmol/mol for N<sub>2</sub>+He+Ar in H<sub>2</sub> Grade E-3, 5 μmol/mol and 50 μmol/mol for O<sub>2</sub> in H<sub>2</sub> Grade  
24 A and B and E-3 respectively, 5 μmol/mol are permitted in H<sub>2</sub> Grade A and B while moisture  
25 should not condense at any ambient conditions in H<sub>2</sub> Grade E-3. NH<sub>3</sub> is produced when the  
26 hydrolysis was performed in NH<sub>4</sub>Cl (reaction (2) and section 3.1). Based on the hydrolysis  
27 results, 1 ml of NH<sub>3</sub> per liter of gas is produced exceeding the permitted limit (0.1 ppm = 0.1  
28 mL/L) according to the ISO standard 14687:2019. Nitrogen and oxygen originate from air  
29 present in the hydrolysis reactor. In the following, a semi-quantitative analysis of CO<sub>2</sub>, CO and

1 CH<sub>4</sub> content (section 3.2.1) and the humidity (section 3.2.2) of the gas mixture obtained after the  
2 hydrolysis of Mg-Ni-G in each of the temperature-solution composition conditions is detailed.

3

### 4 3.2.1. Gas chromatography analysis

5 The variation of CO<sub>2</sub>, CO and CH<sub>4</sub> content was evaluated by micro-GC analysis on the as-  
6 produced gas mixture without adding external standards. For this reason, the results were  
7 considered as semi-quantitative. The gaseous composition of the air was considered as reference.  
8 H<sub>2</sub>, O<sub>2</sub>, N<sub>2</sub> and CO are separated using the MS column with retention time ( $t_R$ ) of 0.6 minutes  
9 (min), 0.8 min, 1.1 min, 1.6 min and 2.0 min respectively while the PPQ column splits up CO<sub>2</sub>  
10 and N<sub>2</sub> at  $t_R = 0.3$  min and 0.4 min respectively.



11  
12 Figure 4: Chromatograms of a) Air (the arrows highlights the position of the peaks attributed to all tested  
13 gases) and gaseous mixture obtained after the hydrolysis of Mg-Ni-G, at various temperatures (*i.e.* 0°C,

1 25°C, 35°C, 45°C and 60°C), in b) NaCl, c) NH<sub>4</sub>Cl and d) HCl using the PPQ and MS columns in  
2 parallel. The insets show the variation of the intensities of CO<sub>2</sub> peak.

3

4 Figure 4.a shows the chromatograms of air obtained after separation in both columns as well as  
5 the position of the peaks of the potentially produced gases. In all cases (regardless the  
6 temperature and the hydrolysis solution), no peaks attributed to CO and CH<sub>4</sub> were observed  
7 indicating that either CO and CH<sub>4</sub> are not produced or their concentration is so low that the  
8 variation of their concentration cannot be estimated. The chromatograms of hydrogen mixture  
9 generated by the hydrolysis in NaCl, NH<sub>4</sub>Cl and HCl are presented in Figures 4.b, 4.c and 4.d  
10 respectively. Only peaks attributed to H<sub>2</sub>, N<sub>2</sub>, O<sub>2</sub> and CO<sub>2</sub> are observed while H<sub>2</sub>O was  
11 eliminated by the protection column installed before the MS and the PPQ columns. H<sub>2</sub> produced  
12 during hydrolysis is mixed with air present in the hydrolysis reactor before the test. With that  
13 being said, the ratio of the peak area A(X) implying the concentration of O<sub>2</sub> over that of N<sub>2</sub> is  
14 constant ( $\frac{A(O_2)}{A(N_2)} \approx 0.33$ ) so that it can be considered as standard for the evaluation of CO<sub>2</sub> amount  
15 variation.

16 The variation of CO<sub>2</sub> amount can be deducted comparing the amount of CO<sub>2</sub> in each hydrogen  
17 mixture to that in air by taking O<sub>2</sub> or N<sub>2</sub> as internal standards. Considering A(CO<sub>2</sub>) as the peak  
18 area of CO<sub>2</sub> and A(X) that of X ( X = O<sub>2</sub>, N<sub>2</sub>) in the same gas mixture, A(CO<sub>2</sub>)/A(X) was  
19 estimated for each mixture. For better comparison, the ratio  $f(CO_2/X)$  is used to determine the  
20 variation of the concentration of CO<sub>2</sub> and it is calculated as follows:

$$f\left(\frac{CO_2}{X}\right) = \frac{\left(\frac{A(CO_2)}{A(X)}\right)_{hydrolysis}}{\left(\frac{A(CO_2)}{A(X)}\right)_{air}} (\%) \quad (5)$$

21 where A(CO<sub>2</sub>) is the peak area of CO<sub>2</sub>, A(X) (X = O<sub>2</sub>, N<sub>2</sub>) is the peak area of the considered  
22 standard, “hydrolysis” designates the corresponding peak area in the gas mixture collected  
23 during the hydrolysis reaction and “air” labels the corresponding peak area in air.  $f(CO_2/O_2)$ ,  $f$   
24  $(CO_2/N_2)$  and  $f(O_2/N_2)$  fractions are shown in Table 2.

25

1 Table 2:  $f(\text{CO}_2/\text{X})$  ( $\text{X} = \text{O}_2, \text{N}_2$ ) and  $f(\text{O}_2/\text{N}_2)$  calculated as mentioned in section 3.2.1 for each condition  
 2 of the hydrolysis solution and temperature.

Hydrolysis solution	Temperature (°C)	$f(\text{CO}_2/\text{X})$ (%)	$f(\text{O}_2/\text{N}_2)$ (%)
NaCl	0	53.6	99.8
	25	14.5	99.7
	35	16.9	99.9
	45	32.3	100.0
	60	42.0	99.9
NH <sub>4</sub> Cl	0	62.4	99.9
	25	28.9	100.0
	35	34.6	99.5
	45	35.1	99.9
	60	69.4	99.8
HCl	0	96.3	99.9
	25	79.2	99.6
	35	95.2	99.8
	45	101.2	99.6
	60	128.9	99.9

3

4  $f(\text{O}_2/\text{N}_2)$  was calculated to verify the quality of the semi-quantitative analysis. The values closed  
 5 to 100% demonstrate that  $\text{O}_2$  and  $\text{N}_2$  from air can be considered as internal standard for the  
 6 analysis of  $\text{CO}_2$  amount in the hydrogen mixture collected during the hydrolysis as mentioned  
 7 above (Table 2). The difference between  $f(\text{CO}_2/\text{O}_2)$  and  $f(\text{CO}_2/\text{N}_2)$  is insignificant so that  $f$   
 8 ( $\text{CO}_2/\text{X}$ ) will be used for the comparison in the following.

9 For instance, an  $f(\text{CO}_2/\text{X})$  greater than 100% indicates that the  $\text{CO}_2$  amount in the hydrolysis gas  
 10 is higher than that in air which is only explained by the production of  $\text{CO}_2$ . While an  $f(\text{CO}_2/\text{X})$   
 11 lower than 100% points out that  $\text{CO}_2$  is consumed during the hydrolysis. This can be attributed to  
 12 the dissolution of  $\text{CO}_2$  in water moisture (the humidity in the hydrogen is discussed in section  
 13 3.2.2) resulting in the possible formation of carbonic acid  $\text{H}_2\text{CO}_3$  (Teramura et al., 2017;  
 14 Wilhelm et al., 1977).

15 As described previously, in order to collect the hydrogen gas produced in the hydrolysis reactor,  
 16 the pressure should be higher than the atmospheric pressure so that the gases pass through the

1 sampling bags. At 0°C, the reaction kinetics are relatively slow and consequently the amount of  
2 gases collected in the sampling bags is lower. Then, the high values of  $f(\text{CO}_2/\text{X})$  at 0°C  
3 (compared to those at 25°C) may be attributed to the poor hydrolysis performance of Mg-Ni-G  
4 as described previously (see Section 3.1 and Figures 3.a, 3.b and 3.c). In addition, the CO<sub>2</sub>  
5 concentration may be affected by the hydrolysis kinetics where CO<sub>2</sub> amount is higher in the gas  
6 mixture obtained by the hydrolysis at higher temperature. This hypothesis is justified by  
7 comparing  $f(\text{CO}_2/\text{X})$  in NaCl, NH<sub>4</sub>Cl and HCl where the highest values were estimated in HCl  
8 followed by NH<sub>4</sub>Cl and NaCl. The highest  $f(\text{CO}_2/\text{X})$  (128.93%) is observed in H<sub>2</sub> produced by  
9 the hydrolysis using HCl solution at 60 °C (more severe hydrolysis conditions). These results  
10 suggest that, when the exothermicity of the reaction increases (*i.e.* extra heat is dissipated), CO<sub>2</sub>  
11 may be produced by the reaction of graphite (ball milling additive) with the oxygen from air. In  
12 fact, this reaction is thermodynamically favorable compared to the formation of CO and CH<sub>4</sub>  
13 since the enthalpy of formation of CO<sub>2</sub> (-393.52 kJ/mol) is lower than that of CO (-110.53  
14 kJ/mol) and CH<sub>4</sub> (-74.87 kJ/mol) respectively (Chase et al., 1998).

15

### 16 3.2.2. Gas mixture humidity

17 Gas mixture humidity is one of the factors affecting the performance of energy systems based on  
18 hydrogen consumption. The excess of water content in hydrogen affects the performance and  
19 durability of proton exchange membrane fuel cells (PEMFC) (Wang et al., 2020; Zhang et al.,  
20 2017) and may reduce flame properties in internal combustion engine (in similarity to  
21 convention fuels) (Awad et al., 2018; White et al., 2006).

22 The humidity of the hydrogen produced by hydrolysis originates mainly from the evaporation of  
23 water due to the exothermicity of the reaction. In the following, the molar ratio of Mg over water  
24 is defined by  $R_h$  (*i.e.*  $R_h = \frac{n(\text{Mg})}{n(\text{H}_2\text{O})}$ ). In order to validate this hypothesis, the mass of the powder  
25 placed in the hydrolysis reactor was varied to 100 mg ( $R_h = 3.3 \times 10^{-3}$ ), 200 mg ( $R_h = 6.7 \times 10^{-3}$ )  
26 and 400 mg ( $R_h = 13.3 \times 10^{-3}$ ) while retaining the same volume of solution (20 mL, still in large  
27 excess). In an adiabatic system and assuming that the heat capacity of the system is conserved,

1 the overall enthalpy of the reaction ( $\Delta H$ ) is proportional to the mass of the powder which  
2 increases the temperature of the media according to the equation:

$$\Delta H = n_{Mg} \times \Delta_r H = C_p \times \Delta T \quad (6)$$

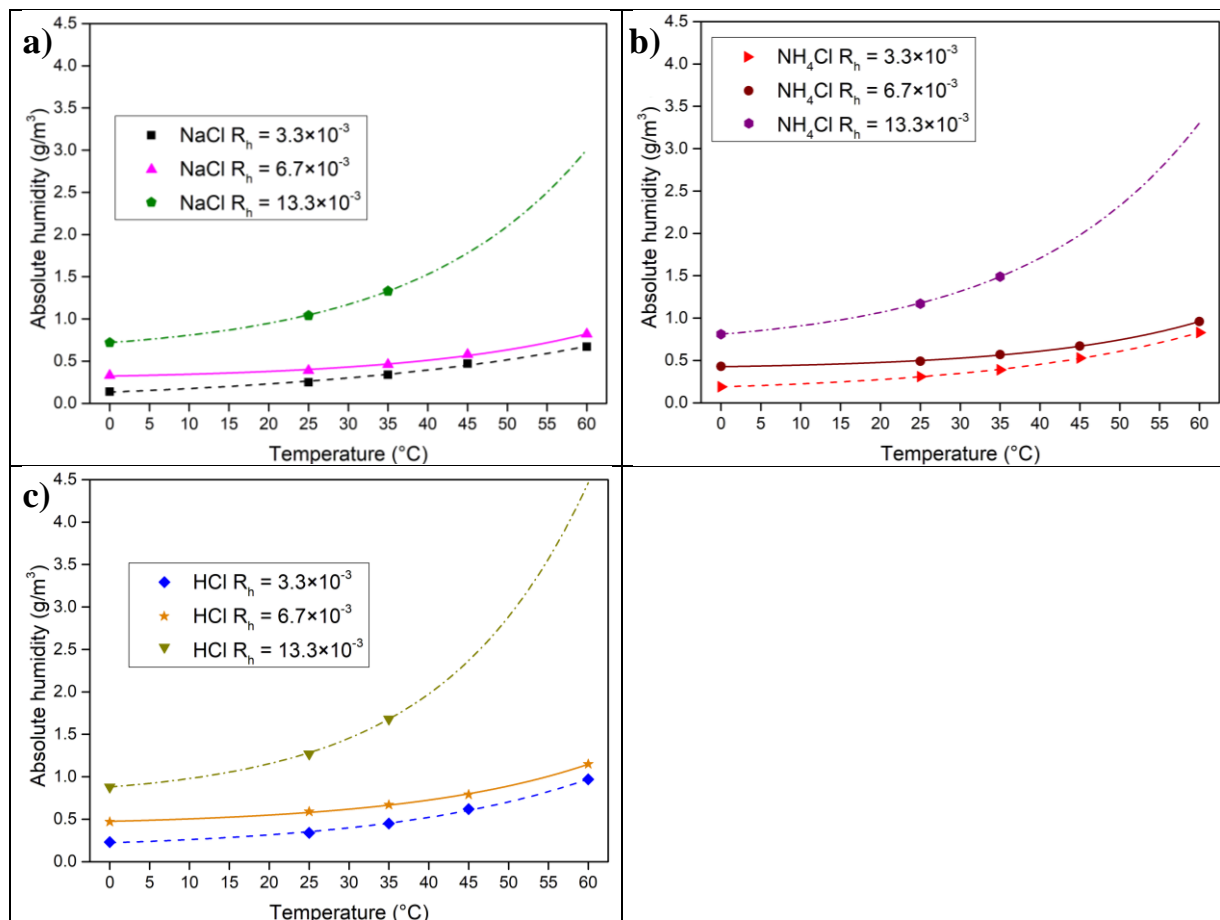
3 where  $n_{Mg}$  is the number of moles of Mg,  $\Delta_r H$  is the molar reaction enthalpy (-354 kJ/mol (Al  
4 Bacha et al., 2019)),  $C_p$  is the heat capacity of the system and  $\Delta T$  is the change of temperature.

5 In order to investigate the moisture in hydrogen produced during hydrolysis of Mg, the absolute  
6 humidity (hereby referred to as AH, equation 7) in hydrogen produced while varying  $R_h$ , the  
7 temperature of the reaction media and the hydrolysis solution was estimated.

$$AH = \frac{m(H_2O)}{V_{net}} \quad (7)$$

8 where  $m(H_2O)$  is the mass of water vapor in g and  $V_{net}$  is the volume of the measuring system  
9 (hydrogen + water vapor) in  $m^3$ .

10



1

2 Figure 5: Absolute humidity of the hydrogen produced by the hydrolysis of Mg-Ni-G, for R<sub>h</sub> values of  
 3 3.3 × 10<sup>-3</sup>, 6.7 × 10<sup>-3</sup> and 13.3 × 10<sup>-3</sup>, in a) NaCl, b) NH<sub>4</sub>Cl and c) HCl solutions.

4 Figures 5.a, 5.b and 5.c show the maximal absolute humidity (AH) measured in hydrogen  
 5 produced by the hydrolysis of Mg-Ni-G at different R<sub>h</sub> in NaCl, NH<sub>4</sub>Cl and HCl respectively.  
 6 For instance, at 25 °C and for R<sub>h</sub> = 6.7 × 10<sup>-3</sup>, AH of hydrogen produced by the hydrolysis in HCl  
 7 is 0.57 g/m<sup>3</sup> (equivalent to 0.57 ppm or 0.57 μmol/mol) compared to 0.42 g/m<sup>3</sup> and 0.36 g/m<sup>3</sup> for  
 8 NH<sub>4</sub>Cl and NaCl respectively. For the reaction carried out with R<sub>h</sub> = 13.3 × 10<sup>-3</sup> at 45 °C and 60 °C,  
 9 the sudden and quick hydrogen production reaction increases the pressure and consequently the  
 10 leaks in the low-pressure hydrogen generation system. The experimental results were fitted using  
 11 an empirical exponential-type equation (8):

$$AH = \alpha e^{\beta T} \quad (8)$$

12 As expected, hydrogen produced by the hydrolysis in HCl is moister than that produced by the  
 13 hydrolysis in NH<sub>4</sub>Cl and NaCl respectively. This is attributed to the fact that the hydrolysis

1 performance of Mg-Ni-G are maximal in HCl solution (section 3.1) because of the exothermicity  
2 of the reaction increases the reaction media temperature and evaporates water from the solution.  
3 Moreover, the absolute humidity grows up with increasing the reaction media temperature from  
4 0°C to 60°C. In the latter case, increasing the reaction temperature induces a higher water  
5 evaporation from the hydrolysis solution and hydrolysis performances amelioration (Figures 3.a,  
6 3.b and 3.c, section 3.1) with extra heat generated.

7 The effect of the exothermicity of the reaction is relevant by comparing the absolute humidity of  
8 hydrogen at different  $R_h$  values. Note that the higher  $R_h$ , the greater the enthalpy of the reaction  
9 (the reaction is more exothermic and more extra heat is generated). In all cases, the  
10 exothermicity of the reaction was found to have a major impact on the humidity of hydrogen  
11 where the highest AH values were measured when  $R_h = 13.3 \times 10^{-3}$  ( $m_{\text{powder}} = 400$  mg and  $V_{\text{solution}}$   
12  $= 20$  mL) while the lowest AH values were recorded when  $R_h = 3.3 \times 10^{-3}$  ( $m_{\text{powder}} = 100$  mg and  
13  $V_{\text{solution}} = 20$  mL).

14

#### 15 **4. Conclusion**

16 Hydrogen production by the hydrolysis reaction of Mg-based materials was reported to be a  
17 promising method for hydrogen on demand systems. The hydrolysis performances (*i.e.* yield and  
18 kinetics) are influenced by different reactions conditions such as the composition of the powder,  
19 the composition of the solution and the reaction temperature.

20 The reaction performances obtained in 0.6 mol/L NaCl (*i.e.* average concentration of NaCl in  
21 seawater) were compared to those obtained in 0.6 mol/L  $\text{NH}_4\text{Cl}$  and 0.6 mol/L HCl. Lowering  
22 the pH of the solution by replacing NaCl with weak acid  $\text{NH}_4\text{Cl}$  and strong acid HCl improves  
23 the kinetics of the reaction due to the dissolution of the passivation layer of  $\text{Mg}(\text{OH})_2$ . The  
24 activation energy determined from Avrami-Erofeev equation decreases with the initial pH of the  
25 solution. Indeed,  $E_A$  decreases from 15.06 kJ/mol, for the hydrolysis of Mg-Ni-G in NaCl, to  
26 6.86 kJ/mol in HCl solution. The “excess” production of gas (*i.e.* yield greater than 100%)  
27 during the hydrolysis in  $\text{NH}_4\text{Cl}$  is assigned to the production of  $\text{NH}_3$ .

1 Moreover, the composition of the hydrogen mixture obtained during the hydrolysis has been  
2 analyzed by micro-GC and hygrometric measurements. Regardless the hydrolysis solution  
3 composition, no CO or CH<sub>4</sub> were detected during the gas mixture analysis. In contrast, the semi-  
4 quantitative chromatography analysis showed that, in severe hydrolysis conditions, the  
5 concentration of CO<sub>2</sub> in the gas mixture is higher than that in air inducing the graphite oxidation  
6 into carbon dioxide CO<sub>2</sub> during the hydrolysis process.

7 Considering the gas mixture composition, the absolute humidity is higher when:

- 8 - the pH of the hydrolysis solution is minimal (*i.e.* strong acid HCl is used as hydrolysis  
9 solution),
- 10 - the temperature of the hydrolysis reaction media increases (T = 60 °C) and
- 11 - the heat generated by the reaction is higher ( $R_h = 13.3 \times 10^{-3}$ ).

12 The hydrolysis of Mg-Ni-G is complete in less than 5 minutes regardless the chloride solution at  
13 ambient temperature. However, many aspects have to be taken into consideration such as the cost,  
14 the durability of the reactor and the purity required for the fuel utilization. The use of acids (*i.e.*  
15 NH<sub>4</sub>Cl and HCl) is only advantageous in term of kinetics. On the contrary, the two media  
16 promote the production of CO<sub>2</sub>, increase the humidity and affect the durability of the reactor by  
17 enhancing its corrosion. Moreover, the production of NH<sub>3</sub> during the hydrolysis in NH<sub>4</sub>Cl  
18 solution is harmful to the PEMFC. Then, the use of seawater (*i.e.* 0.6 mol/L NaCl) appears as the  
19 best compromise as hydrolysis solution.

20 The present work confirms that the hydrolysis of Mg-based materials in seawater is a clean  
21 (zero-carbon-emission) hydrogen production technique. It can be hoped that our results will  
22 inspire scientists and technicians to investigate whether the hydrogen produced by the hydrolysis  
23 of Mg-based materials meets the requirement of the ISO standard 14687:2019 to fuel energy  
24 production system or not. Moreover, additional analysis must be carried out to highlight the  
25 effect of the amount of hydrogen on the dilution of CO<sub>2</sub> to verify if its permitted limit (*i.e.* 2  
26 ppm) can be achieved. Our results are considered as the start point for other researchers to prove  
27 the efficiency of the hydrolysis reaction as a clean hydrogen production technic.

## 1 **Acknowledgments**

2 This work was financially supported by the AZM & SAADE Association, the Lebanese  
3 University (Scientific research support program), the Lebanese Council of Scientific Research  
4 (CNRSL) and Bordeaux University foundation. The authors thank Guillaume AUBERT and  
5 Cyrielle FAUVEAU for technical assistant with micro-GC analysis.

6

## 7 **Highlights**

- 8 1. Lowering the hydrolysis solution pH enhances the hydrolysis performance.
- 9 2. In HCl solution, the hydrolysis activation energy is reduced to 6.86 kJ/mol.
- 10 3. The humidity of hydrogen is affected by the exothermicity of the reaction.
- 11 4. Graphite is oxidized when extra heat is generated in the reaction media.
- 12 5. Mg-based hydrolysis is a clean hydrogen production technique.

## 1 Bibliography

- 2 Abdin, Z., Zafaranloo, A., Rafiee, A., Mérida, W., Lipiński, W., Khalilpour, K.R., 2020.  
3 Hydrogen as an energy vector. *Renewable and Sustainable Energy Reviews* 120,  
4 109620. <https://doi.org/10.1016/j.rser.2019.109620>
- 5 Abe, J.O., Popoola, A.P.I., Ajenifuja, E., Popoola, O.M., 2019. Hydrogen energy, economy and  
6 storage: Review and recommendation. *International Journal of Hydrogen Energy* 44(29), 15072-  
7 15086. <https://doi.org/10.1016/j.ijhydene.2019.04.068>
- 8 Acar, C., Dincer, I., 2019. Review and evaluation of hydrogen production options for better  
9 environment. *Journal of Cleaner Production* 218, 835-  
10 849. <https://doi.org/10.1016/j.jclepro.2019.02.046>
- 11 Al Bacha, S., Aubert, I., Zakhour, M., Nakhl, M., Bobet, J.L., 2020a. Hydrogen production by  
12 the hydrolysis of ball milled AZ91 (Electrochemical approach), *Journal of Magnesium and*  
13 *Alloys*.
- 14 Al Bacha, S., Awad, A.S., El Asmar, E., Tayeh, T., Bobet, J.L., Nakhl, M., Zakhour, M., 2019.  
15 Hydrogen generation via hydrolysis of ball milled WE43 magnesium waste. *International Journal*  
16 *of Hydrogen Energy* 44(33), 17515-17524. <https://doi.org/10.1016/j.ijhydene.2019.05.123>
- 17 Al Bacha, S., Pighin, S.A., Urretavizcaya, G., Zakhour, M., Castro, F.J., Nakhl, M., Bobet, J.-L.,  
18 2020b. Hydrogen generation from ball milled Mg alloy waste by hydrolysis reaction. *Journal of*  
19 *Power Sources* 479, 228711. <https://doi.org/10.1016/j.jpowsour.2020.228711>
- 20 Al Bacha, S., Pighin, S.A., Urretavizcaya, G., Zakhour, M., Nakhl, M., Castro, F.J., Bobet, J.L.,  
21 2020c. Effect of ball milling strategy (milling device for scaling-up) on the hydrolysis  
22 performance of Mg alloy waste. *International Journal of Hydrogen Energy* 45(41), 20883-  
23 20893. <https://doi.org/10.1016/j.ijhydene.2020.05.214>
- 24 Al Bacha, S., Zakhour, M., Nakhl, M., Bobet, J.L., 2020d. Effect of ball milling in presence of  
25 additives (Graphite, AlCl<sub>3</sub>, MgCl<sub>2</sub> and NaCl) on the hydrolysis performances of Mg<sub>17</sub>Al<sub>12</sub>.  
26 *International Journal of Hydrogen Energy* 45(11), 6102-  
27 6109. <https://doi.org/10.1016/j.ijhydene.2019.12.162>
- 28 Awad, A.S., El-Asmar, E., Tayeh, T., Mauvy, F., Nakhl, M., Zakhour, M., Bobet, J.L., 2016.  
29 Effect of carbons (G and CFs), TM (Ni, Fe and Al) and oxides (Nb<sub>2</sub>O<sub>5</sub> and V<sub>2</sub>O<sub>5</sub>) on hydrogen  
30 generation from ball milled Mg-based hydrolysis reaction for fuel cell. *Energy* 95, 175-  
31 186. <https://doi.org/10.1016/j.energy.2015.12.004>
- 32 Awad, O.I., Ali, O.M., Hammid, A.T., Mamat, R., 2018. Impact of fusel oil moisture reduction  
33 on the fuel properties and combustion characteristics of SI engine fueled with gasoline-fusel oil  
34 blends. *Renewable Energy* 123, 79-91. <https://doi.org/10.1016/j.renene.2018.02.019>
- 35 Buryakovskaya, O.A., Vlaskin, M.S., Ryzhkova, S.S., 2019. Hydrogen production properties of  
36 magnesium and magnesium-based materials at low temperatures in reaction with aqueous

1 solutions. Journal of Alloys and Compounds 785, 136-  
2 145.<https://doi.org/10.1016/j.jallcom.2019.01.003>

3 Chase, M.W., National Institute of S., Technology, 1998. NIST-JANAF thermochemical tables.  
4 American Chemical Society ; American Institute of Physics for the National Institute of  
5 Standards and Technology, [Washington, D.C.]; Woodbury, N.Y.

6 Dawood, F., Anda, M., Shafiullah, G.M., 2020. Hydrogen production for energy: An overview.  
7 International Journal of Hydrogen Energy 45(7), 3847-  
8 3869.<https://doi.org/10.1016/j.ijhydene.2019.12.059>

9 Dincer, I., 2012. Green methods for hydrogen production. International Journal of Hydrogen  
10 Energy 37(2), 1954-1971.<https://doi.org/10.1016/j.ijhydene.2011.03.173>

11 Durbin, D.J., Malardier-Jugroot, C., 2013. Review of hydrogen storage techniques for on board  
12 vehicle applications. International Journal of Hydrogen Energy 38(34), 14595-  
13 14617.<https://doi.org/10.1016/j.ijhydene.2013.07.058>

14 Fuster, V., Castro, F.J., Troiani, H., Urretavizcaya, G., 2011. Characterization of graphite  
15 catalytic effect in reactively ball-milled MgH<sub>2</sub>-C and Mg-C composites. International Journal of  
16 Hydrogen Energy 36(15), 9051-9061.<https://doi.org/10.1016/j.ijhydene.2011.04.153>

17 Grosjean, M.-H., Roué, L., 2006. Hydrolysis of Mg-salt and MgH<sub>2</sub>-salt mixtures prepared by  
18 ball milling for hydrogen production. Journal of Alloys and Compounds 416(1), 296-  
19 302.<https://doi.org/10.1016/j.jallcom.2005.09.008>

20 Grosjean, M.H., Zidoune, M., Roué, L., 2005. Hydrogen production from highly corroding Mg-  
21 based materials elaborated by ball milling. Journal of Alloys and Compounds 404-406, 712-  
22 715.<https://doi.org/10.1016/j.jallcom.2004.10.098>

23 Grosjean, M.H., Zidoune, M., Roué, L., Huot, J.Y., 2006. Hydrogen production via hydrolysis  
24 reaction from ball-milled Mg-based materials. International Journal of Hydrogen Energy 31(1),  
25 109-119.<https://doi.org/10.1016/j.ijhydene.2005.01.001>

26 Hiraki, T., Hiroi, S., Akashi, T., Okinaka, N., Akiyama, T., 2012. Chemical equilibrium analysis  
27 for hydrolysis of magnesium hydride to generate hydrogen. International Journal of Hydrogen  
28 Energy 37(17), 12114-12119.<https://doi.org/10.1016/j.ijhydene.2012.06.012>

29 Hou, X., Wang, Y., Yang, Y., Hu, R., Yang, G., Feng, L., Suo, G., Ye, X., Zhang, L., Shi, H.,  
30 Yang, L., Chen, Z.-G., 2019. Enhanced hydrogen generation behaviors and hydrolysis  
31 thermodynamics of as-cast Mg-Ni-Ce magnesium-rich alloys in simulate seawater. International  
32 Journal of Hydrogen Energy 44(44), 24086-  
33 24097.<https://doi.org/10.1016/j.ijhydene.2019.07.148>

34 Huang, M., Ouyang, L., Wang, H., Liu, J., Zhu, M., 2015. Hydrogen generation by hydrolysis of  
35 MgH<sub>2</sub> and enhanced kinetics performance of ammonium chloride introducing. International  
36 Journal of Hydrogen Energy 40(18), 6145-6150.<https://doi.org/10.1016/j.ijhydene.2015.03.058>

- 1 Huang, M., Ouyang, L., Ye, J., Liu, J., Yao, X., Wang, H., Shao, H., Zhu, M., 2017. Hydrogen  
2 generation via hydrolysis of magnesium with seawater using Mo, MoO<sub>2</sub>, MoO<sub>3</sub> and MoS<sub>2</sub> as  
3 catalysts. *Journal of Materials Chemistry A* 5(18), 8566-  
4 8575.<https://doi.org/10.1039/C7TA02457F>
- 5 ISO, 2019. Hydrogen fuel quality — Product specification, ISO 14687. p. 14687.
- 6 Kravchenko, O.V., Sevastyanova, L.G., Urvanov, S.A., Bulychev, B.M., 2014. Formation of  
7 hydrogen from oxidation of Mg, Mg alloys and mixture with Ni, Co, Cu and Fe in aqueous salt  
8 solutions. *International Journal of Hydrogen Energy* 39(11), 5522-  
9 5527.<https://doi.org/10.1016/j.ijhydene.2014.01.181>
- 10 Kushch, S.D., Kuyunko, N.S., Nazarov, R.S., Tarasov, B.P., 2011. Hydrogen-generating  
11 compositions based on magnesium. *International Journal of Hydrogen Energy* 36(1), 1321-  
12 1325.<https://doi.org/10.1016/j.ijhydene.2010.06.115>
- 13 Liu, C.-H., Chen, B.-H., Hsueh, C.-L., Ku, J.-R., Tsau, F., Hwang, K.-J., 2009. Preparation of  
14 magnetic cobalt-based catalyst for hydrogen generation from alkaline NaBH<sub>4</sub> solution. *Applied*  
15 *Catalysis B: Environmental* 91(1-2), 368-379.<https://doi.org/10.1016/j.apcatb.2009.06.003>
- 16 Ma, M., Yang, L., Ouyang, L., Shao, H., Zhu, M., 2019. Promoting hydrogen generation from  
17 the hydrolysis of Mg-Graphite composites by plasma-assisted milling. *Energy* 167, 1205-  
18 1211.<https://doi.org/10.1016/j.energy.2018.11.029>
- 19 Marbán, G., Valdés-Solís, T., 2007. Towards the hydrogen economy? *International Journal of*  
20 *Hydrogen Energy* 32(12), 1625-1637.<https://doi.org/10.1016/j.ijhydene.2006.12.017>
- 21 Mauvy, F., Bobet, J.-I., Sabatier, J., Bos, F., 2019. Use of a magnesium-based material for  
22 producing dihydrogen or electricity. Google Patents, France, p. 27.
- 23 Mazloomi, K., Gomes, C., 2012. Hydrogen as an energy carrier: Prospects and challenges.  
24 *Renewable and Sustainable Energy Reviews* 16(5), 3024-  
25 3033.<https://doi.org/10.1016/j.rser.2012.02.028>
- 26 Midilli, A., Ay, M., Dincer, I., Rosen, M.A., 2005. On hydrogen and hydrogen energy strategies:  
27 I: current status and needs. *Renewable and Sustainable Energy Reviews* 9(3), 255-  
28 271.<https://doi.org/10.1016/j.rser.2004.05.003>
- 29 Nikolaidis, P., Poullikkas, A., 2017. A comparative overview of hydrogen production processes.  
30 *Renewable and Sustainable Energy Reviews* 67, 597-  
31 611.<https://doi.org/10.1016/j.rser.2016.09.044>
- 32 Öz, Ç., Coşkuner Filiz, B., Kantürk Figen, A., 2017. The effect of vinegar–acetic acid solution  
33 on the hydrogen generation performance of mechanochemically modified Magnesium (Mg)  
34 granules. *Energy* 127, 328-334.<https://doi.org/10.1016/j.energy.2017.03.106>

- 1 Pighin, S.A., Urretavizcaya, G., Bobet, J.L., Castro, F.J., 2020 Nanostructured Mg for hydrogen  
2 production by hydrolysis obtained by MgH<sub>2</sub> milling and dehydriding. Journal of Alloys and  
3 Compounds 827, 154000.<https://doi.org/10.1016/j.jallcom.2020.154000>
- 4 Pinsky, M.L., Takano, K., 2004. Chapter 8 - Property Estimation for Electrolyte Systems, in:  
5 Kontogeorgis, G.M., Gani, R. (Eds.), Computer Aided Chemical Engineering. Elsevier, pp. 181-  
6 204.
- 7 Potapov, S.N., Gvozdkov, I.A., Belyaev, V.A., Verbetsky, V.N., Mitrokhin, S.V., 2019.  
8 Magnesium hydride based hydrogen chemical source: Development and application perspectives.  
9 International Journal of Hydrogen Energy 44(54), 28578-  
10 28585.<https://doi.org/10.1016/j.ijhydene.2019.09.094>
- 11 Pourbaix, M., 1974. Atlas of Electrochemical Equilibria in Aqueous Solutions NATIONAL  
12 ASSOCIATION of CORROSION ENGINEERS, Houston, Texas, USA.
- 13 Qu, Z.Y., Wang, F., Liu, P., Yu, Q.L., Brouwers, H.J.H., 2020. Super-hydrophobic magnesium  
14 oxychloride cement (MOC): from structural control to self-cleaning property evaluation.  
15 Materials and Structures 53(2), 30.<https://doi.org/10.1617/s11527-020-01462-3>
- 16 Radcliffe, J.C., 2018. The water energy nexus in Australia – The outcome of two crises. Water-  
17 Energy Nexus 1(1), 66-85.<https://doi.org/10.1016/j.wen.2018.07.003>
- 18 Rand, D.A.J., 2011. A journey on the electrochemical road to sustainability. Journal of Solid  
19 State Electrochemistry 15(7-8), 1579-1622.<https://doi.org/10.1007/s10008-011-1410-z>
- 20 Rusman, N.A.A., Dahari, M., 2016. A review on the current progress of metal hydrides material  
21 for solid-state hydrogen storage applications. International Journal of Hydrogen Energy 41(28),  
22 12108-12126.<https://doi.org/10.1016/j.ijhydene.2016.05.244>
- 23 Sabatier, J., Mauvy, F., Bobet, J.-L., Mohedano, D., Faessel, M., Bos, F., 2018. A New Device  
24 for Hydrogen Production on Demand with Application to Electric Assist Bike: Description,  
25 Production Characteristics and Basic Control, 15th International Conference on Informatics in  
26 Control, Automation and Robotics. Porto, Portugal, pp. 411-419.
- 27 Seyam, S., Dincer, I., Agelin-Chaab, M., 2020. Analysis of a clean hydrogen liquefaction plant  
28 integrated with a geothermal system. Journal of Cleaner Production 243,  
29 118562.<https://doi.org/10.1016/j.jclepro.2019.118562>
- 30 Tan, W., Yang, Y.-e., Fang, Y.-x., 2020. Isothermal hydrogen production behavior and kinetics  
31 of bulk eutectic Mg–Ni-based alloys in NaCl solution. Journal of Alloys and Compounds 826,  
32 152363.<https://doi.org/10.1016/j.jallcom.2019.152363>
- 33 Tan, Z., Ouyang, L., Liu, J., Wang, H., Shao, H., Zhu, M., 2018. Hydrogen generation by  
34 hydrolysis of Mg-Mg<sub>2</sub>Si composite and enhanced kinetics performance from introducing of  
35 MgCl<sub>2</sub> and Si. International Journal of Hydrogen Energy 43(5), 2903-  
36 2912.<https://doi.org/10.1016/j.ijhydene.2017.12.163>

- 1 Tan, Z.H., Ouyang, L.Z., Huang, J.M., Liu, J.W., Wang, H., Shao, H.Y., Zhu, M., 2019.  
2 Hydrogen generation via hydrolysis of Mg<sub>2</sub>Si. *Journal of Alloys and Compounds* 770, 108-  
3 115.<https://doi.org/10.1016/j.jallcom.2018.08.122>
- 4 Tayeh, T., Awad, A.S., Nakhl, M., Zakhour, M., Silvain, J.F., Bobet, J.L., 2014. Production of  
5 hydrogen from magnesium hydrides hydrolysis. *International Journal of Hydrogen Energy* 39(7),  
6 3109-3117.<https://doi.org/10.1016/j.ijhydene.2013.12.082>
- 7 Teramura, K., Hori, K., Terao, Y., Huang, Z., Iguchi, S., Wang, Z., Asakura, H., Hosokawa, S.,  
8 Tanaka, T., 2017. Which is an Intermediate Species for Photocatalytic Conversion of CO<sub>2</sub> by  
9 H<sub>2</sub>O as the Electron Donor: CO<sub>2</sub> Molecule, Carbonic Acid, Bicarbonate, or Carbonate Ions? *The*  
10 *Journal of Physical Chemistry C* 121(16), 8711-8721.<https://doi.org/10.1021/acs.jpcc.6b12809>
- 11 Uan, J.-Y., Yu, S.-H., Lin, M.-C., Chen, L.-F., Lin, H.-I., 2009. Evolution of hydrogen from  
12 magnesium alloy scraps in citric acid-added seawater without catalyst. *International Journal of*  
13 *Hydrogen Energy* 34(15), 6137-6142.<https://doi.org/10.1016/j.ijhydene.2009.05.133>
- 14 Wang, Y., Xie, X., Zhou, C., Feng, Q., Zhou, Y., Yuan, X.-Z., Xu, J., Fan, J., Zeng, L., Li, H.,  
15 Wang, H., 2020. Study of relative humidity on durability of the reversal tolerant proton exchange  
16 membrane fuel cell anode using a segmented cell. *Journal of Power Sources* 449,  
17 227542.<https://doi.org/10.1016/j.jpowsour.2019.227542>
- 18 White, C.M., Steeper, R.R., Lutz, A.E., 2006. The hydrogen-fueled internal combustion engine:  
19 a technical review. *International Journal of Hydrogen Energy* 31(10), 1292-  
20 1305.<https://doi.org/10.1016/j.ijhydene.2005.12.001>
- 21 Wilhelm, E., Battino, R., Wilcock, R.J., 1977. Low-pressure solubility of gases in liquid water.  
22 *Chemical Reviews* 77(2), 219-262.<https://doi.org/10.1021/cr60306a003>
- 23 Xie, X., Ni, C., Wang, B., Zhang, Y., Zhao, X., Liu, L., Wang, B., Du, W., 2020. Recent  
24 advances in hydrogen generation process via hydrolysis of Mg-based materials: A short review.  
25 *Journal of Alloys and Compounds* 816, 152634.<https://doi.org/10.1016/j.jallcom.2019.152634>
- 26 Yu, S.-H., Uan, J.-Y., Hsu, T.-L., 2012. Effects of concentrations of NaCl and organic acid on  
27 generation of hydrogen from magnesium metal scrap. *International Journal of Hydrogen Energy*  
28 37(4), 3033-3040.<https://doi.org/10.1016/j.ijhydene.2011.11.040>
- 29 Zhang, S., Chen, B., Shu, P., Luo, M., Xie, C., Quan, S., Tu, Z., Yu, Y., 2017. Evaluation of  
30 performance enhancement by condensing the anode moisture in a proton exchange membrane  
31 fuel cell stack. *Applied Thermal Engineering* 120, 115-  
32 120.<https://doi.org/10.1016/j.applthermaleng.2017.03.128>

33